CHINESE OPTICS LETTERS
Vol. 19, No. 5 | May 2021

Thermally tunable microfiber knot resonator with flexible graphene heater

Yunzheng Wang (王云征)[1,2,†], Qing Wu (吴 卿)[1,3,†], Huide Wang (王慧德)[1], Jiefeng Liu (刘捷锋)[1], Zheng Zheng (郑 铮)[3,4], Meng Zhang (张 梦)[3*], and Han Zhang (张 晗)[1]

[1] International Collaborative Laboratory of 2D Materials for Optoelectronics Science and Technology of Ministry of Education, Institute of Microscale Optoelectronics, Shenzhen University, Shenzhen 518060, China

[2] Singapore University of Technology and Design, Singapore 487372, Singapore

[3] School of Electronic and Information Engineering, Beihang University, Beijing 100191, China

[4] Beijing Advanced Innovation Center for Big Data-Based Precision Medicine, Beihang University, Beijing 100083, China

*Corresponding author: mengzhang10@buaa.edu.cn
Received August 13, 2020 | Accepted November 20, 2020 | Posted Online February 24, 2021

Efficiently tuning the output intensity of an optical device is of vital importance for the establishment of optical interconnects and networks. Thermo-optical modulation is an easily implemented and convenient approach and has been widely employed in photonic devices. In this paper, we proposed a novel thermo-optical modulator based on a microfiber knot resonator (MKR) and graphene heater. Upon applying voltage to graphene, the resonant property of the MKR could be thermally tuned with a maximum phase shift of 2.1π. Intensity modulation shows a fast optical response time thanks to the high thermal conductivity of graphene and the thin microfiber diameter of the MKR.

Keywords: microfiber knot resonator; graphene heater; thermo-optical modulation.
DOI: 10.3788/COL202119.051301

1. Introduction

Optical modulation has been ubiquitously employed in a variety of photonics and opto-electronics application fields, including optical communication, medical engineering, environmental sensing, and security defense[1,2]. As one of the most significant devices in optical networks, optical modulators are showing great appeal to many emerging internet applications, e.g., cloud computing, big data, and internet of things[3]. Compared with traditional electronic interconnect methods, optical modulators possess many important advantages of high bandwidth and low loss and consequently attract intense research interest. Different types of optical modulators have been successfully demonstrated based on various optical effects of materials, such as all-optical[4,5], electro-optical[6,7], and thermo-optical modulators[8,9]. Among these, thermo-optical modulators offer advantages in terms of easy implementation, low cost, and potential applications in optical routing and switching[1]. Traditional metal heaters have difficulty being integrated on non-planar micro- and nanostructures owing to their poor flexibility and large insertion loss caused by excess light absorption. One viable solution is to utilize graphene as a transparent flexible heater for thermally tuning optical modulators[8,10,11].

Since the first, to the best of our knowledge, exfoliation of single-layer graphene in 2004[12], graphene has attracted extensive interest and been widely used in diverse fields due to its excellent electronic, thermal, and photonic properties[13–15]. Benefiting from its unique atomic structure, graphene has linear dispersion of electrons, ultrafast carrier mobility, high mechanical strength, and strong light–matter interaction[16–18]. Especially, its deformable lattice structure brings good flexibility, making it very suitable for non-planar nanostructures. Its high transparency avoids large insertion loss when being integrated with optical structures. More importantly, graphene has extraordinarily high thermal conductivity of $5300\,\mathrm{W/(m\cdot K)}$[19], which will greatly reduce the response time of optical devices based on the thermo-optic effect due to better thermal management ability[20,21]. In recent years, based on the sheet resistance property and high thermal conductivity of graphene, several thermo-optical modulators have been demonstrated using graphene as a transparent flexible heater[10,20]. However, they were all fabricated utilizing a complicated and expensive semiconductor technology, e.g., lithography. Compared with silicon optical waveguides, microfibers have attracted considerable attention due to their outstanding optical and mechanical properties, such as ease of fabrication, low loss, and strong field confinement[22,23]. The microfiber knot resonator (MKR), manufactured by knotting a microfiber into a ring, has lots of prominent advantages such as flexible configurability, compact size, good environmental stability, and low cost[24–26]. It has been successfully used in all-optical modulators, sensors, optical buffers, and logic gates[27–30].

In this contribution, a graphene-MKR thermo-optical modulator was proposed based on the sheet resistance and high thermal conductivity of graphene. The graphene with ~19 layers was synthesized by the chemical vapor deposition (CVD) method and transferred onto interdigital electrodes by the wet-transfer technique. The MKR was prepared by knotting a 2 μm diameter microfiber into a ring, and a partial microfiber ring was adhered to the graphene. The MKR was demonstrated to have a considerable resonant property for optical modulation. By applying voltage to graphene, the proposed thermo-optical modulator could achieve phase modulation and intensity modulation with large modulation depth, large conversion efficiency, and fast response speed. It is expected that our research results will bring new highlights to graphene-based thermo-optical modulators and have great potential in optical communications.

2. Preparation of Graphene-MKR Device

The schematic diagram of the proposed graphene-MKR modulator is shown in Fig. 1(a), which consists of three parts: interdigital electrodes, graphene thin film, and MKR. The interdigital electrodes are deposited on a silicon–silica substrate and covered by a graphene thin film. An MKR is placed on the top of the graphene thin film. When external voltage is applied to the graphene thin film by the interdigital electrodes, a large amount of joule heat will be generated in the graphene thin film and then transferred to the MKR. This changes the refractive index of the MKR owing to thermo-optic effect and further tunes the resonant wavelength of the MKR by affecting the resonant conditions. On the basis of this, phase modulation and intensity modulation can be achieved when guiding narrow band and broad band light into the MKR, respectively.

The detailed fabrication processes are schematically depicted in Figs. 1(b)–1(d). Firstly, a silicon wafer covered with 300 nm silica was selected as a substrate to manufacture the modulator [Fig. 1(b)]. A patterned 40-nm-thick Au layer was deposited on the silica by the thermal evaporation method for interdigital electrodes [Fig. 1(c)]. To enhance the adhesion of the Au layer, a 10-nm-thick Cr layer was introduced between them by the metal mask method in advance. Then, a piece of few-layer graphene thin film was transferred onto the interdigital electrodes by a wet-transfer technique [Fig. 1(d)]. Specifically, the few-layer graphene was grown on a 50-μm-thick copper foil by CVD and uniformly coated by polymethyl methacrylate (PMMA) using a spin coater. After PMMA naturally dried, the whole PMMA-graphene-copper structure was cut into $1\,\mathrm{cm} \times 1\,\mathrm{cm}$ squares and immersed in ammonium persulfate solution to etch away the copper substrate. The remained PMMA-graphene was repetitiously rinsed in deionized (DI) water to remove the etchant residue, transferred to the interdigital electrodes on a microscopic platform, and dried at 40°C–60°C for 2 h to ensure better adhesion between graphene and interdigital electrodes. Subsequently, the device was soaked with acetone to remove the PMMA, and the acetone was rinsed out with ethanol, leaving only few-layer graphene on the interdigital electrodes. Finally, the graphene-MKR modulator was assembled by fixing a home-made MKR on the silicon–silica substrate and contacting the ring of the MKR with the few-layer graphene [Fig. 1(a)]. Specifically, a microfiber with a diameter of ~2 μm was fabricated by flame-heating and tapering a single mode fiber without a coating layer and then knotted into an MKR whose ring diameter was measured to be ~552 μm [see Fig. 1(h)]. In addition, the

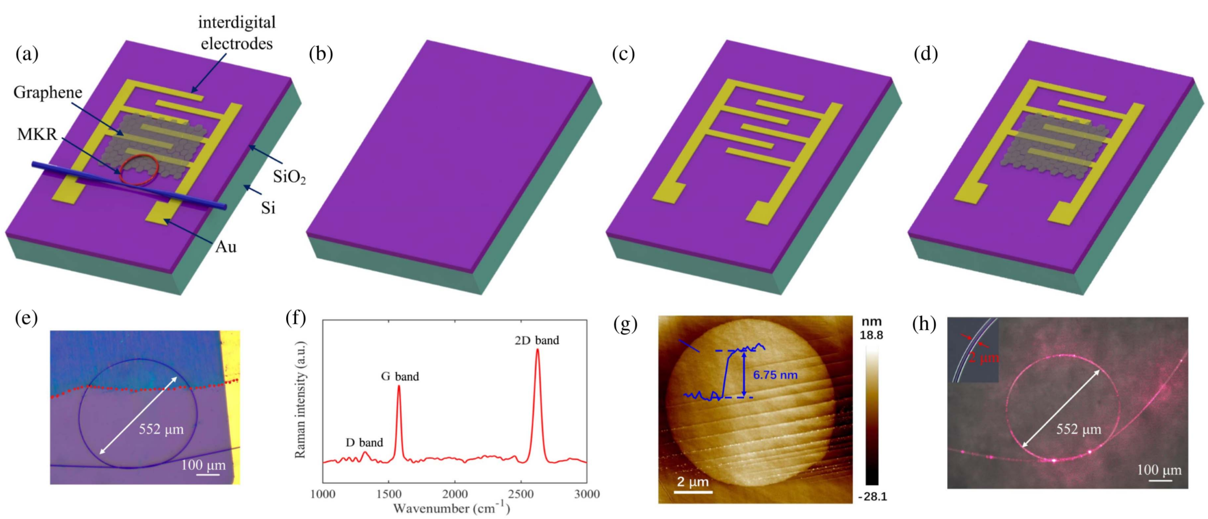

Fig. 1. (a) Schematic diagram of the proposed graphene-MKR modulator. (b)–(d) Detailed fabrication processes. (e) Optical microscopic image of fabricated graphene-MKR modulator. (f) Raman spectrum of CVD-grown graphene. (g) AFM image. (h) Optical microscope images of MKR illuminated by a red laser and microfiber (inset).

insertion loss of the MKR is measured to be ~2.75 dB at 1550 nm and ~3.13 dB at 980 nm. Figure 1(e) shows the optical microscopic image of the fabricated graphene-MKR modulator.

Figure 1(f) displays the Raman spectrum of CVD-grown graphene, which exhibits three characteristic peaks at 1322 cm^{-1} (D band), 1577 cm^{-1} (G band), and 2627 cm^{-1} [two-dimensional (2D) band]. The relatively weak D band indicates that the graphene has low density of defects and high crystallinity. The atomic force microscopy (AFM) image [Fig. 1(g)] shows the morphology of the graphene with the thickness measured to be ~6.75 nm, corresponding to ~20 layers[31].

3. Graphene-MKR Modulator

The proposed graphene-MKR modulator could be employed to achieve phase modulation and intensity modulation when guiding narrowband and broadband light into the MKR, respectively. Figure 2(a) gives the experimental setup when the modulator serves as a phase modulation device. A wide spectrum amplified spontaneous emission (ASE) source was selected to be the incident light source. The transmission spectrum was monitored by an optical spectrum analyzer (OSA, Yokogawa AQ6370D). An electric voltage source was connected to the interdigital electrodes.

The resonant phenomenon of the MKR comes from the circulation of partial incident light in the ring and the interference between the circulating light and output light. The resonant properties of the MKR were checked by measuring its transmission spectrum, shown in Fig. 2(b). It is clear that there are many dips in the spectrum, each of which corresponds to a resonant wavelength. The resonant wavelength λ_{res} could be expressed as

$$\lambda_{res} = 2\pi R n_{eff}/m, \quad (1)$$

where R is the ring radius of the MKR, n_{eff} is the effective refractive index of the microfiber, and $m = 1, 2, 3, \ldots$ is the resonant order[32–34]. Assuming $n_{eff} = 1.48$, the resonant order m is

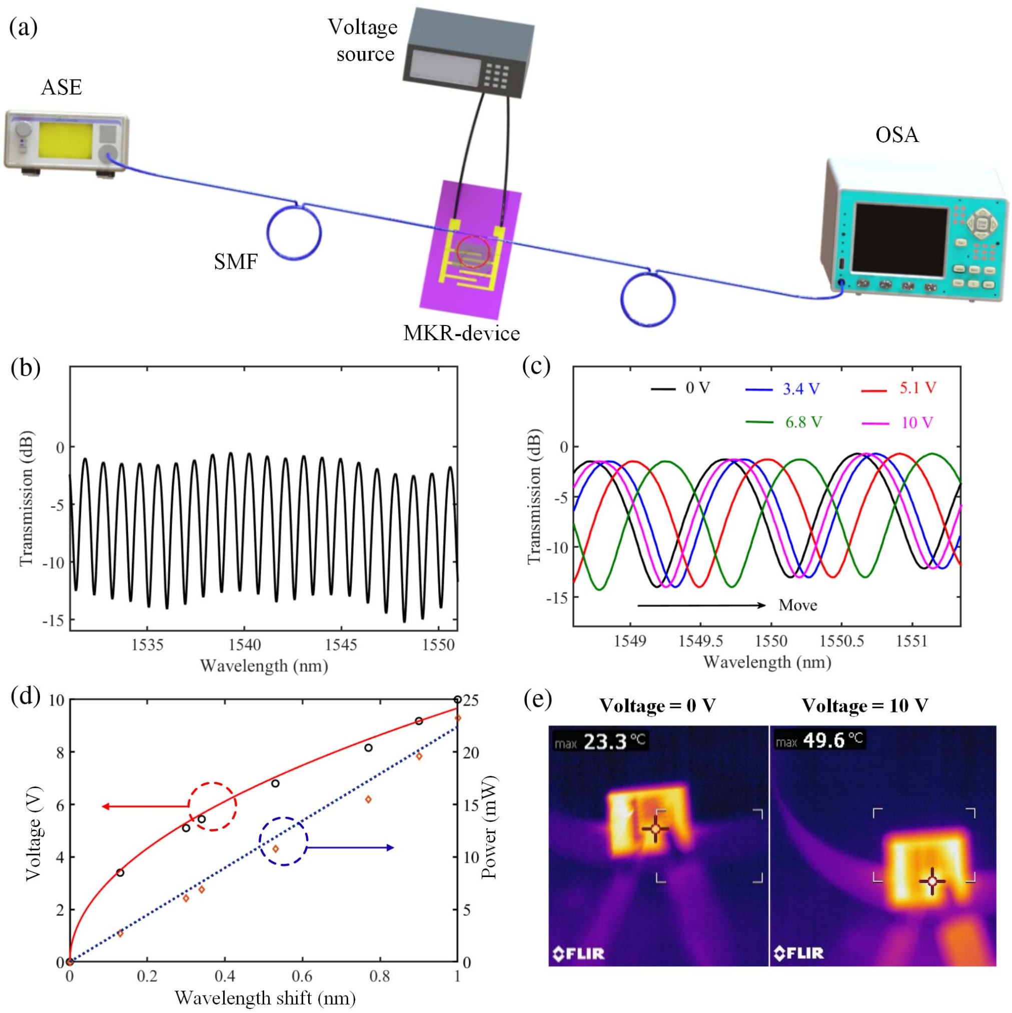

Fig. 2. (a) Experimental setup of phase modulation system based on the graphene-MKR modulator. ASE, amplified spontaneous emission; SMF, single mode fiber; OSA, optical spectrum analyzer. (b) Typical transmission spectrum. (c) Transmission spectra under different voltages. (d) The dependence of spectral shift on voltage and electric power. (e) Thermograms of the graphene-MKR modulator at 0 V (left) and 10 V (right).

calculated to be as large as 3311 at $\lambda_{res} = 1550.12$ nm. Additionally, the free spectral range of the MKR could be written as $\lambda_{FSR} = \lambda^2/(2\pi R\, n_{eff})$, where λ is the vacuum wavelength. For the MKR with ring diameter of ~552 μm, λ_{FSR} is calculated to be ~0.936 nm, which is consistent with the measurement result of 0.938 nm. At $\lambda_{res} = 1549.19$ nm, the extinction ratio, the quality factor, and the fineness are measured to be ~13.4 dB, 4339, and 2.6, respectively. These characteristics indicate that the prepared graphene-MKR structure has a considerable resonant property and is suitable for optical modulation.

According to Eq. (1), it could be easily concluded that the resonant wavelength λ_{res} changes with the effective refractive index n_{eff}. In experiment, by applying voltage to graphene, a large amount of joule heat is generated in graphene and then transferred to the MKR due to the high thermal conductivity of graphene. This changes the refractive index of the MKR by the thermo-optic effect and further tunes the resonant wavelength of the MKR by affecting the resonant conditions[33]. Figure 2(c) shows the typical transmission spectra measured at 0 V, 3.4 V, 5.1 V, 6.8 V, and 10 V, corresponding to the spectral shift (phase shift) of 0 nm (0π), 0.13 nm (0.28π), 0.3 nm (0.64π), 0.53 nm (1.13π), and 1 nm (2.13π), respectively. The transmission spectrum moves towards the longer wavelength direction as the voltage increases, which results from the fact that the thermo-optic coefficient of the silica fiber is a positive value ($\sim 1.1\times 10^{-5}\ \mathrm{K}^{-1}$)[9].

The variation of the spectral shift as a function of voltage is shown in Fig. 2(d), which could be well fitted by a quadratic function. From Eq. (1), by ignoring the influence of the thermal expansion effect of microfiber, the relationship between the spectral shift ($\Delta\lambda$) and the temperature variation (ΔT) can be written as

$$\Delta\lambda = \frac{\lambda_{res}}{n_{eff}} \times \frac{dn}{dT} \times \Delta T, \tag{2}$$

where dn/dT is the thermo-optic coefficient of the microfiber. The temperature variation ΔT is proportional to the applied electric power. Therefore, the spectral shift $\Delta\lambda$ has a quadratic relation with the applied voltage U as

$$\Delta\lambda \propto U^2/R', \tag{3}$$

where R' represents the total resistance, which includes the sheet resistance of graphene, the sheet resistance of metal electrodes, and the contact resistance of the metal-graphene interface, and was measured to be ~4.3 kΩ in the experiment. Figure 2(d) also clearly depicts the linear relation between spectral shift $\Delta\lambda$ and electric power. The conversion efficiency is calculated to be 0.288 rad/mW, larger than results in previously reported modulators[33,35].

To further verify that a large amount of joule heat was generated in graphene while applying the voltage, the temperature variation was observed by an infrared thermal camera (FLIR E60). Figure 2(e) shows the recorded thermograms at 0 V and 10 V. Obvious temperature rises from 23.3°C to 49.6°C could be easily recognized, proving the above standpoints. Besides, although metal electrodes generate a certain amount

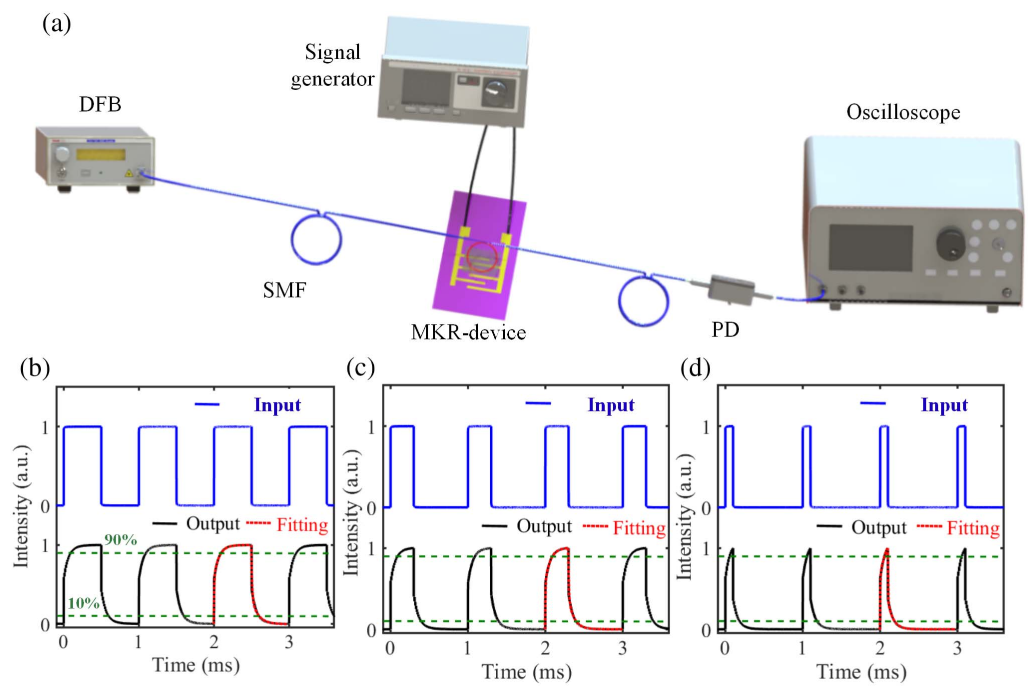

Fig. 3. (a) Experimental setup of the optical switch system based on the graphene-MKR modulator. DFB, distributed feedback laser; SMF, single mode fiber. (b)–(d) Waveforms of input voltage (up, blue) and output light (down, black) measured at duty cycle of 50:50, 30:70, and 10:90, respectively. Red lines represent the fitting curves of rising and falling edges of output light waveforms.

of heat, it hardly has any effect on modulation of the MKR device because of the large distance between it and the MKR [see Fig. 1(e)].

Upon guiding a narrowband light beam into the MKR, the graphene-MKR modulator can be used to achieve intensity modulation as an optical switch. The operation principle of the optical switch can be depicted as follows: when the light wavelength is near the resonant wavelength of MKR, the output light intensity will be very weak; when the light wavelength is far away from the resonant wavelength of MKR, the output light intensity will be large; therefore, the output light intensity could be controlled through tuning the resonant wavelength of the MKR by applying different voltages to graphene. Figure 3(a) shows the experimental setup of the optical switch. Different from Fig. 2(a), the light source was served by a distributed feedback laser (DFB) to provide a narrowband continuous-wave laser beam, and the output light was monitored by a photodetector (Thorlabs DET08CFC/M) and an oscilloscope (Keysight DSOS104A). In addition, the voltage source was an arbitrary waveform generator (TFG6940A) that was used to supply a voltage signal with variable amplitude, frequency, and duty cycle.

Figure 3(b) shows the typical waveforms of input voltage and output light. The input voltage has a frequency of 1000 Hz, a voltage amplitude of 10 V, and a duty cycle of 50%. A clear ON-OFF switch of output light intensity indicates that the input light was successfully modulated and possessed the same frequency and duty cycle as the input voltage. Due to the slow response of heat generation and dissipation, the waveforms of the output light have slightly smooth edges compared with those of input voltage. Fitting these edges by exponential functions gives the time constants of the rising edge and falling edge to be 41.1 μs and 41.2 μs, respectively. According to the 10%–90% rule, the rise/fall time is evaluated to be 90.8 μs/89.7 μs, which is ~2.2 times the exponential rising/falling time constant, consistent with the theoretical result. Benefiting from the excellent environmental stability of MKR, the output light waveform could remain unchanged for a long time. Waveforms at a duty cycle of 30:70 and 10:90 are shown in Figs. 3(c) and 3(d), which have similar rising/falling time as that in Fig. 3(b). Obvious switch characteristics remain well at duty cycle of 10:90, suggesting that the modulation rate of the graphene-MKR modulator can be increased.

4. Conclusion

In summary, a graphene-MKR thermo-optical modulator was proposed by taking advantage of the sheet resistance property and high thermal conductivity of graphene. The graphene was fabricated by the CVD method and characterized to have ~19 layers. After being applied external electric voltage, graphene generates a large amount of heat, which changes the resonant property of MKR owing to thermo-optical effect. Based on this change, phase modulation and intensity modulation were successfully achieved. For phase modulation, the maximum phase shift was 2.1π at the available highest voltage of 10 V, and the modulation depth was as large as 13.4 dB. For intensity modulation, a short response time of ~41 μs was obtained with long-term stability. We believe that the proposed graphene-MKR thermo-optical modulator with advantages of easy implementation, low cost, high modulation efficiency, large modulation depth, and fast response speed will promote the development of 2D materials-based modulators towards optical communication and networks.

Acknowledgement

M. Zhang acknowledges the support from the National Natural Science Foundation of China (NSFC) (Nos. 51778030 and 51978024). H. Zhang acknowledges the support from the State Key Research Development Program of China (No. 2019YFB2203503), NSFC (Nos. 61875138, 61435010, and 61961136001), and Science and Technology Innovation Commission of Shenzhen (Nos. KQTD2015032416270385, JCYJ20170811093453105, JCYJ20180307164612205, and GJHZ20180928160209731). The authors also acknowledge the support from the Instrumental Analysis Center of Shenzhen University (Xili Campus).

†These authors contributed equally to this work.

References

1. Z. P. Sun, A. Martinez, and F. Wang, "Optical modulators with 2D layered materials," Nat. Photon. **10**, 227 (2016).
2. C. T. Phare, Y.-H. D. Lee, J. Cardenas, and M. Lipson, "Graphene electro-optic modulator with 30 GHz bandwidth," Nat. Photon. **9**, 511 (2015).
3. G. T. Reed, G. Mashanovich, F. Y. Gardes, and D. J. Thomson, "Silicon optical modulators," Nat. Photon. **4**, 518 (2010).
4. Q. Wu, S. Chen, Y. Wang, L. Wu, X. Jiang, F. Zhang, X. Jin, Q. Jiang, Z. Zheng, J. Li, M. Zhang, and H. Zhang, "MZI-based all-optical modulator using MXene $Ti_3C_2T_x$ (T = F, O, or OH) deposited microfiber," Adv. Mater. Technol. **4**, 1800532 (2019).
5. Y. Wang, W. Huang, C. Wang, J. Guo, F. Zhang, Y. Song, Y. Ge, L. Wu, J. Liu, J. Li, and H. Zhang, "An all-optical, actively Q-switched fiber laser by an antimonene-based optical modulator," Laser Photon. Rev. **13**, 1800313 (2019).
6. M. Liu, X. Yin, E. Ulin-Avila, B. Geng, T. Zentgraf, L. Ju, F. Wang, and X. Zhang, "A graphene-based broadband optical modulator," Nature **474**, 64 (2011).
7. Y. Ding, X. Guan, X. Zhu, H. Hu, S. I. Bozhevolnyi, L. K. Oxenlowe, K. J. Jin, N. A. Mortensen, and S. Xiao, "Efficient electro-optic modulation in low-loss graphene-plasmonic slot waveguides," Nanoscale **9**, 15576 (2017).
8. J. T. Kim, K. H. Chung, and C. G. Choi, "Thermo-optic mode extinction modulator based on graphene plasmonic waveguide," Opt. Express **21**, 15280 (2013).
9. K. Wu, Y. F. Wang, C. Y. Qiu, and J. P. Chen, "Thermo-optic all-optical devices based on two-dimensional materials," Photon. Res. **6**, C22 (2018).
10. L. H. Yu, Y. L. Yin, Y. C. Shi, D. X. Dai, and S. L. He, "Thermally tunable silicon photonic microdisk resonator with transparent graphene nanoheaters," Optica **3**, 159 (2016).
11. S. Gan, C. Cheng, Y. Zhan, B. Huang, X. Gan, S. Li, S. Lin, X. Li, J. Zhao, H. Chen, and Q. Bao, "A highly efficient thermo-optic microring modulator assisted by graphene," Nanoscale **7**, 20249 (2015).
12. K. S. Novoselov, A. K. Geim, S. V. Morozov, D. Jiang, Y. Zhang, S. V. Dubonos, I. V. Grigorieva, and A. A. Firsov, "Electric field effect in atomically thin carbon films," Science **306**, 666 (2004).

13. Q. Bao, H. Zhang, Y. Wang, Z. Ni, Y. Yan, Z. X. Shen, K. P. Loh, and D. Y. Tang, "Atomic-layer graphene as a saturable absorber for ultrafast pulsed lasers," Adv. Funct. Mater. **19**, 3077 (2009).
14. H. Jiang, Y. Tang, X. Zeng, R. Xiao, P. Lü, L. Wang, and Y. Lu, "Visual measurement of the microscopic temperature of porous graphene based on cholesteric liquid crystal microcapsules," Chin. Opt. Lett. **18**, 031201 (2020).
15. C. Zhao, Q. Huang, M. A. Araimi, A. Rozhin, S. Sergeyev, and C. Mou, "Observation of chaotic polarization attractors from a graphene mode locked soliton fiber laser," Chin. Opt. Lett. **17**, 020012 (2019).
16. K. I. Bolotin, K. J. Sikes, Z. Jiang, M. Klima, G. Fudenberg, J. Hone, P. Kim, and H. L. Stormer, "Ultrahigh electron mobility in suspended graphene," Solid State Commun. **146**, 351 (2008).
17. Q. Bao and K. P. Loh, "Graphene photonics, plasmonics, and broadband optoelectronic devices," ACS Nano **6**, 3677 (2012).
18. F. Bonaccorso, Z. Sun, T. Hasan, and A. C. Ferrari, "Graphene photonics and optoelectronics," Nat. Photon. **4**, 611 (2010).
19. A. A. Balandin, S. Ghosh, W. Bao, I. Calizo, D. Teweldebrhan, F. Miao, and C. N. Lau, "Superior thermal conductivity of single-layer graphene," Nano Lett. **8**, 902 (2008).
20. L. H. Yu, D. X. Dai, and S. L. He, "Graphene-based transparent flexible heat conductor for thermally tuning nanophotonic integrated devices," Appl. Phys. Lett. **105**, 251104 (2014).
21. A. A. Balandin, "Thermal properties of graphene and nanostructured carbon materials," Nat. Mater. **10**, 569 (2011).
22. Y. Yu, Q. Bian, N. Zhang, Y. Lu, X. Zhang, and J. Yang, "Investigation on an all-optical intensity modulator based on an optical microfiber coupler," Chin. Opt. Lett. **16**, 040605 (2018).
23. J. Y. Lou, Y. P. Wang, and L. M. Tong, "Microfiber optical sensors: a review," Sensors **14**, 5823 (2014).
24. P. Wang, Y. P. Wang, and L. M. Tong, "Functionalized polymer nanofibers: a versatile platform for manipulating light at the nanoscale," Light-Sci. Appl. **2**, e102 (2013).
25. L. M. Tong, "Micro/nanofibre optical sensors: challenges and prospects," Sensors **18**, 903 (2018).
26. C. Meng, Y. Xiao, P. Wang, L. Zhang, Y. X. Liu, and L. M. Tong, "Quantum-dot-doped polymer nanofibers for optical sensing," Adv. Mater. **23**, 3770 (2011).
27. Y. D. Wang, X. T. Gan, C. Y. Zhao, L. Fang, D. Mao, Y. P. Xu, F. L. Zhang, T. L. Xi, L. Y. Ren, and J. L. Zhao, "All-optical control of microfiber resonator by graphene's photothermal effect," Appl. Phys. Lett. **108**, 171905 (2016).
28. L. T. Gai, J. Li, and Y. Zhao, "Preparation and application of microfiber resonant ring sensors: a review," Opt. Laser Technol. **89**, 126 (2017).
29. M. Bahadoran, A. Afroozeh, J. Ali, and P. P. Yupapin, "Slow light generation using microring resonators for optical buffer application," Opt. Eng. **51**, 044601 (2012).
30. A. Godbole, P. P. Dali, V. Janyani, T. Tanabe, and G. Singh, "All optical scalable logic gates using Si_3N_4 microring resonators," IEEE J. Sel. Top. Quantum Electron. **22**, 5900308 (2016).
31. F. S. Al-Hazmi, G. W. Beall, A. A. Al-Ghamdi, A. Alshahrie, F. S. Shokr, and W. E. Mahmoud, "Raman and ellipsometry spectroscopic analysis of graphene films grown directly on Si substrate via CVD technique for estimating the graphene atomic planes number," J. Mol. Struct. **1118**, 275 (2016).
32. W. Bogaerts, P. De Heyn, T. Van Vaerenbergh, K. De Vos, S. K. Selvaraja, T. Claes, P. Dumon, P. Bienstman, D. Van Thourhout, and R. Baets, "Silicon microring resonators," Laser Photon. Rev. **6**, 47 (2012).
33. C. Qiu, Y. Yang, C. Li, Y. Wang, K. Wu, and J. Chen, "All-optical control of light on a graphene-on-silicon nitride chip using thermo-optic effect," Sci. Rep. **7**, 17046 (2017).
34. L. F. Stokes, M. Chodorow, and H. J. Shaw, "All-single-mode fiber resonator," Opt. Lett. **7**, 288 (1982).
35. S.-C. Yan, B.-C. Zheng, J.-H. Chen, F. Xu, and Y.-Q. Lu, "Optical electrical current sensor utilizing a graphene-microfiber-integrated coil resonator," Appl. Phys. Lett. **107**, 053502 (2015).